EI SEVIER

Contents lists available at ScienceDirect

Scripta Materialia

journal homepage: www.elsevier.com/locate/scriptamat



CrossMark

Regular Article

Pt surface segregation in L1₀-FePt nano-grains

H. Sepehri-Amin ^{a,*}, H. Iwama ^b, G. Hrkac ^c, K.T. Butler ^d, T. Shima ^b, K. Hono ^{a,1}

- ^a Research Center for Magentic and Spintronic Materials, National Institute for Materials Science, Tsukuba 305-0047, Japan
- ^b Faculty of Engineering, Tohoku Gakuin University, Tagajo 985-8537, Japan
- ^c University of Exeter, UK
- d University of Bath, UK

ARTICLE INFO

Article history: Received 22 February 2017 Received in revised form 27 March 2017 Accepted 27 March 2017 Available online xxxx

Keywords: FePt Microstructure Surface segregation Atomistic simulation

ABSTRACT

The influence of the chemical compositions of FePt films on the surface segregations of Pt was investigated by cross-sectional high angle annular dark field (HAADF) scanning transmission electron microscopy (STEM) of $L1_0$ -FePt granular films grown on single crystalline MgO substrates. *Ab initio* atomistic simulations revealed the surface segregation of Pt is detremental for the magentocrystalline anisotropy energy of the $L1_0$ -FePt grains. This detremental effect is pronounced for the grain size of less than 15 nm. We found that the Pt surface segregation can be suppressed by a trace addition of Ag to the FePt film.

© 2017 Acta Materialia Inc. Published by Elsevier Ltd. All rights reserved.

Heat assisted magnetic recording (HAMR) has been considered to be the most promising technology that may substitute the current perpendicular magnetic recording (PMR) method for the next generation hard disk drives with the areal density exceeding 2 Tbit/in². To realize the HAMR technology, L1₀-FePt granular media with a grain size of 4-6 nm are needed [1]. Such a media structure has been demonstrated in the FePt-C system [2-4]. However, the reduction of FePt grain size results in the reduction of the degree of L10 order, which causes the distribution of K_u and switching fields of FePt nanograins [5–7]. Ab-initio calculations and Monte Carlo simulations have shown that the ordering temperature of FePt grains decreases when the grain size reduces [8-12]. Based on the theoretical calculations, this was attributed to the existence of the surface segregation of Pt in the L1₀-FePt grains [10–13]. Experimental studies also confirmed the surface segregation of Pt in the nanosized L1₀-FePt grains [14–16]. The surface segregation of Pt can lead to the compositional deviation in the core region of the L1₀-FePt nanograins from the FePt stoichiometry, which may reduce the degree of L10 order in the FePt grains. In fact, the largest magnetocrystalline anisotropy energy of L1₀-FePt films was reported for Pt-rich compositions [13]. However, it is still not understood how the surface segregation of Pt is influenced by the off-stoichiometry of FePt grains and how it can be eliminated from the L1₀-FePt nanograins. In this work, we have investigated the influence of the chemical compositions of FePt films to the surface segregation in L1₀-FePt grains. We

also found a trace addition of Ag suppress the formation of thick Ptshell in the L1₀-FePt grains.

FePt films with a thickness of 10 nm were prepared by an ultra-high vacuum magnetron co-sputtering system using Fe and Pt targets on polished single crystalline MgO (100) substrate at the substrate temperature of 700 °C and a base pressure better than 8.5×10^{-7} Pa. High-purity argon of 0.2 Pa was introduced during sputtering. The input power for the Pt target was kept constant at 16 W while the input power for the Fe target was varied from 30 W to 35 W to tune Fe to Pt ratio in the films. The compositions of the films were determined to be Fe_{47.2}Pt_{52.8}, Fe_{48.8}Pt_{51.2} and Fe_{51.8}Pt_{48.2} (at.%) by an electron probe Xray microanalysis (EPMA). In the same way, FePt-Ag films were prepared using an ultra-high vacuum magnetron co-sputtering system with separate targets of Fe, Pt and Ag. FePt-Ag layer of 0.43 nm was deposited on MgO (100) substrate at the substrate temperature of 700 °C and consecutively, the FePt layer of 9.57 nm was deposited at 700 °C. The composition of the film was determined to be (Fe_{0.49}Pt_{0.51})_{99.4}Ag_{0.6} (at.%). The magnetic properties of the samples were measured using a superconducting quantum interface device vibrating sample magnetometer (SQUID-VSM) with a maximum applied magnetic field of 7 T. The microstructures of the films were characterized using a Titan G2 80-200 scanning transmission electron microscope (STEM) equipped with a probe aberration corrector. Energy dispersive X-ray spectroscopy (EDS) was collected using a Super-X EDX detector. The specimens for the TEM analyses were prepared by focused ion beam (FEI Nanolab Helios 650) using the lift-out method.

In order to understand the influence of the surface segregation of L1₀-FePt grains to the averaged magnetocrystalline anisotropy constant of the grains, we performed *ab initio* electronic structure calculations of

^{*} Corresponding author.

E-mail address: h.sepehriamin@nims.go.jp (H. Sepehri-Amin).

¹ Dr. Kazuhiro Hono was an editor of the journal during the review period of the article. To avoid a conflict of interest, Prof. Jeff Th.M. De Hosson acted as editor for this manuscript.

magnetocrystalline anistropy energy (MAE) using VASP (plane wave pseudopotential) [17–23]. We modeled Pt or Fe surface segregation on L₁₀-FePt grains with a set of discrete ordered supercells of different sizes, in which symmetrically inequivalent atomic orders were considered. This allows us to investigate the potential effect of local atomic positional distributions of Fe and Pt on MAE and spin moments. For the MAE calculations, we used the VASP plane wave density functional theory code with projector augmented wave pseudopotential [17–23]. In this calculation, we used the collinear and non-collinear spin density functional (Pauli equation) and the genralized gradient approximation (GGA) within the PBE scheme [24–25]. The MAE is very sensitive to the number of k-points used in the Brillouin zone integrations and the k-space interpolation scheme. Therefore we used 21³, 17³ and 7³ Γ -centered k-point meshes for each unit cell in the following 1, 2 \times 2 \times 1 and 3 \times 3 \times 1 unit cell MAE calculations. For the actual MAE calculations, we used two different schemes; one was the total energies for different spin polraization directions E|| and E⊥ calculated independently by separate charge densities in the presence of the spin-orbit term. The spin-orbit term was first neglected and the charge density for both spin orientations was assumed to be equal. E|| and E \perp were calcualted by adding the spin-orbit term as a perturbation, in which Kohn-Sham eigenvalues were converged in its presence. For the perfect unit cell structure without any defects, we have performed a k-point study, as mentioned above, and showed that for a $3\times3\times1$ supercell structure and 21^3 k-point mesh for each unit cell the magnetocrystalline ansiotropy converged from a one unit cell value of 1.82×10^7 J/m 3 to a value of 1.28×10^7 J/m 3 , and a further refinement of the K-point mesh did not lead to a change in magnetocrystalline ansiotropy value.

Fig. 1(a)–(c) show the out-of-plane and in-plane magnetization curves obtained from the FePt films with different composition of Fe $_{47.2}$ Pt $_{52.8}$, Fe $_{48.8}$ Pt $_{51.2}$ and Fe $_{51.8}$ Pt $_{48.2}$ (at.%), respectively. The Ptrich films show similar coercivity values of 5.85 and 5.58 T while the film with Fe-rich composition shows a lower coercivity of 3.21 T.

Note that the slope of in-plane hysteresis loop near 0 T increases for Fe-rich film compare to that of Pt-rich film. The remanent magnetization ratio $M_{r|l}/M_{r^\perp}$ of the films were calculated to be 0.000, 0.060, and 0.062 for the Fe_{47.2}Pt_{52.8}, Fe_{48.8}Pt_{51.2}, and Fe_{51.8}Pt_{48.2} films, respectively. Fig. 1(d)–(f) show plane-view low magnification high angle annular dark field (HAADF) STEM images obtained from the Fe_{47.2}Pt_{52.8}, Fe_{48.8}Pt_{51.2} and Fe_{51.8}Pt_{48.2} films, respectively. The FePt grain size varies from ~10 to ~100 nm for all three films. Fig. 1(g)–(i) show high resolution HAADF-STEM images obtained from the surface of FePt grains in these films.

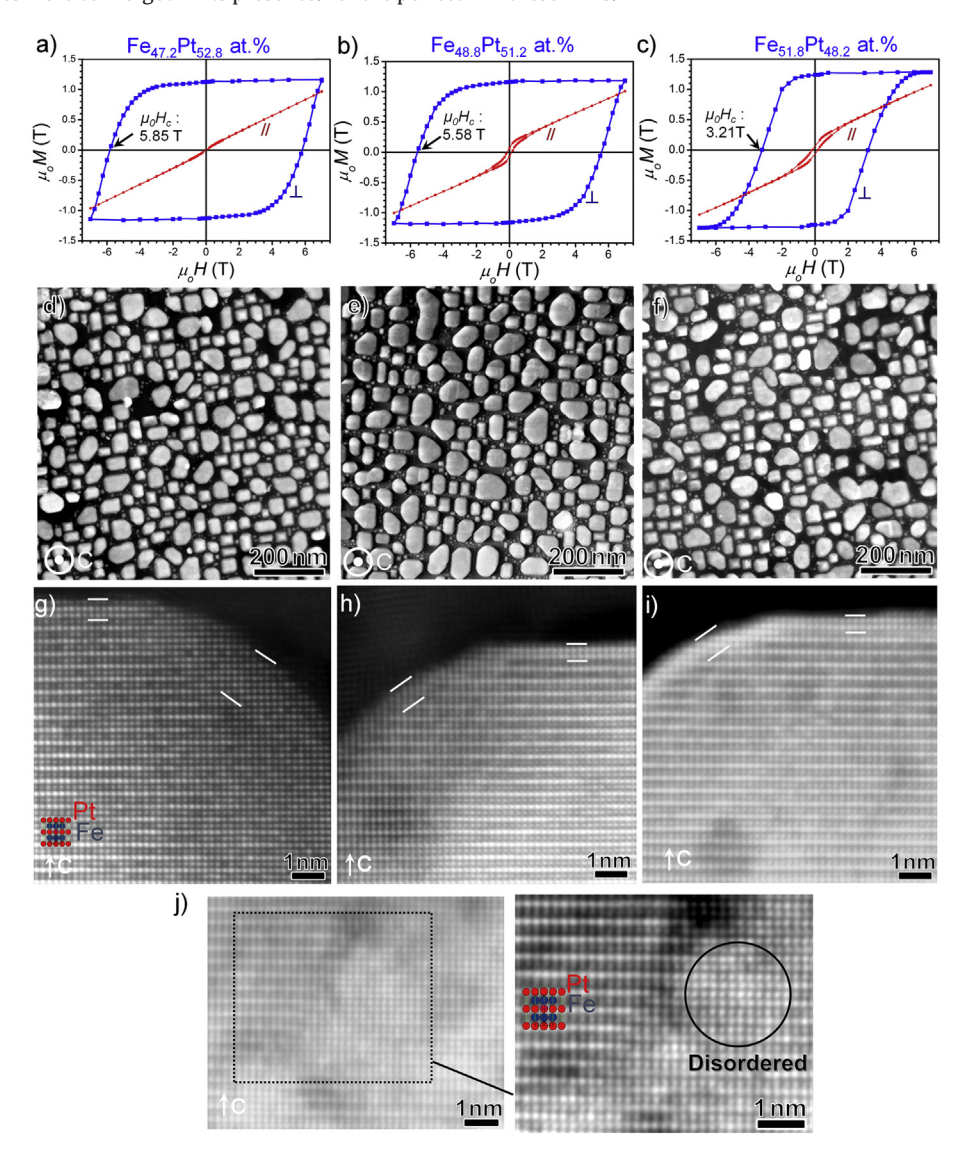


Fig. 1. Out-of-plane and in-plane magnetization curves, plane-view HAADF-STEM, and high resolution HAADF-STEM images obtained from surface of FePt grains of FePt films with different film composition of (a), (d), (g) Fe_{47.2}Pt_{52.8}, (b), (e), (h) Fe_{48.8}Pt_{51.2}, and (c), (f), (i) Fe_{51.8}Pt_{48.2} at.%. (j) Enlarged HAADF-STEM images taken from inside of an FePt grain of film with composition of Fe_{51.8}Pt_{48.2} at.%.

Download English Version:

https://daneshyari.com/en/article/5443373

Download Persian Version:

https://daneshyari.com/article/5443373

<u>Daneshyari.com</u>